First-principles calculations of thermodynamic properties and planar fault energies in Co3X and Ni3X L12 compounds

Breidi, Abed Al Hasan; Allen, Joshua; Mottura, Alessandro

DOI:
10.1002/pssb.201600839

Document Version
Peer reviewed version

Citation for published version (Harvard):
Breidi, AAH, Allen, J & Mottura, A 2017, 'First-principles calculations of thermodynamic properties and planar fault energies in Co3X and Ni3X L12 compounds', *Physica Status Solidi B-Basic Solid State Physics*, vol. 254, no. 9, 1600839. https://doi.org/10.1002/pssb.201600839

First-principles calculations of thermodynamic properties and planar fault energies in Co_3X and Ni_3X $L1_2$ compounds

A. Breidi,* J. Allen, and A. Mottura
School of Metallurgy and Materials, University of Birmingham, Edgbaston B15 2TT, United Kingdom
(Dated: April 3, 2017)

We do Density Functional Theory based total-energy calculations of the $L1_2$ phase in Co_3X and Ni_3X compounds, X being a transition metal element. The lattice parameters, magnetic moments, formation enthalpies, are determined and compared with the available experimental data. The (111) superlattice intrinsic stacking fault energy (SISF), a crucial factor affecting materials strength and their mechanical behavior is calculated using the axial interaction model. We have applied the quasiharmonic Debye model in conjunction with first-principles in order to establish the temperature dependence of the lattice parameters and the (111) SISF energies. We investigate our prediction of a low formation enthalpy in the system Ni-25 at.%Zn by doing auxiliary simulations for the fcc random alloy at the composition 25 at.%Zn. Our simulations indicate that the elements: Ti, Zr, Hf, Nb and Ta can help stabilizing the promising and extremely important $Co_3Al_{0.5}W_{0.5}$ alloy.

I. INTRODUCTION

Superalloys are very significant to a wide array of industries including aerospace[1], nuclear[2] and fossil fuel[3–5]. The main application for these alloys is in turbine blades, as there is a desire for alloys that function in more extreme environments, namely higher temperatures. Superalloys were traditionally based off nickel because of the high temperature strength and creep resistance that derives from the two phase γ/γ' microstructure[6–8]. Older Co based alloys were less successful as they relied on carbides for strengthening[4–6], but the discovery in 2006 by Sato *et al.*[9] of the γ' phase in the Co_3(Al,W) system has led to a renewed interest in Co based alloys which have the potential to be used at higher temperatures and to experience greater creep[10] and oxidation resistance[5]. A greater understanding of the consequences of adding solutes to Co and Ni based alloys is necessary in order to improve their mechanical properties such as increasing planar fault energies, as well as increasing the γ' solvus temperature as this is the upper limit in operating temperature in these alloys[3,11,12].

Despite the fact that the lattice parameters and the formation enthalpies of the stable $L1_2$ phases in cobalt and nickel based compounds are available in the literature, there is no systematic calculation of these properties for the whole set of these compounds. In fact, most of the 3, 4, and 5*d* elements are used in superalloys as solutes. A possible dependence of the formation enthalpies and lattice parameters on the position of the element in the periodic table can be helpful in understanding the role of a given element, when added as an alloying element, on affecting these properties in alloys.

The knowledge of the geometrical stacking fault energies, known as *superlattice intrinsic stacking fault* (SISF) energies is of prime interest since they consist together with antiphase boundary (APB) and complex stacking fault (CSF) energies an indespensable set of values, where the relative difference in magnitude between these fault energies controls the equilibrium configuration of glissile superlattice dislocations and the relative stability of different dissocciation modes, which in turn have the strongest impact on the mechanical behaviour of $L1_2$ compounds[13].

There are two main ways to assess stacking fault energies (SFE), the first is by the use of experimentation and the second is by the use of first-principles density functional theory (DFT) simulations[14,15]. Experimental measurements are typically conducted by measuring the width of the stacking fault ribbon. Considering that the width of this ribbon is inversely proportional to the fault energy[5,16,17], this technique

is typically fraught with difficulties such as: (a) thin film effects, (b) short length ribbons can be comparable to the errors, (c) uncertainty about how to apply corrections, and (d) dislocations can interact with other dislocations resulting in non-equilibrium scenarios[13,18–20].

The abovementioned measurement problematics are not encountered with first-principles simulations. DFT-based simulations have the advantage that they can be used to compute wide variety of properties for phases that are metastable. In addition, they are characterized by high accuracy[21,22].

Within the context of a larger study, we investigate in this paper the variation of the ground state properties *i.e.*, lattice parameter, magnetic moment, formation enthalpies, and (111) SISF in Co_3X and Ni_3X $L1_2$ compounds, where X belongs to most of $3d$ (Ti through Zn), $4d$ (Zr through Cd), and $5d$ (Hf through Hg). We do spin-polarized (SP) and spin-restricted (non spin-polarized – non-SP) calculations. Our simulations demonstrate the instrumental role of magnetism in rendering $L1_2$ compounds stable or unstable.

The paper is organized as follows: the next section (II) presents the calculating methodology and the first-principles technique. In section III we present and discuss the ground state properties: lattice parameter, magnetic moment, and formation enthalpies. In section IV, the (111) SISF formation energies of selected systems are presented and discussed. In section V we conclude, highlighting key outcomes from the new results.

II. COMPUTATIONAL METHOD

A. Methodology: Axial Interaction Model

The AIM model is used to calculate the energy of a structure of N close packed planes[17,23]. According to this model, each plane is assigned a value of a spin variable S_i, where the layer at $(i+1)$ assumes the value of $+1$ (known as spin up) if it follows the nature stacking sequence, otherwise a value of -1 (spin down). This allows the total energy of the system (E) to be defined using the following expansion[17]

$$E = J_0 - J_1 \sum_i S_i S_{i+1} - J_2 \sum_i S_i S_{i+2} - J_3 \sum_i S_i S_{i+3} - J_4 \sum_i S_i S_{i+4} - ..., \quad (1)$$

where the $J's$ are expansion coefficients. The occurence of a stacking fault causes a layer or a series of layers to deviate from the original stacking sequence[10,17,24], for example the formation of an Intrinsic Stacking fault (ISF) in the (111) plane of an FCC structure leads to the stacking sequence ABCACABC. The energy of the faulted structure can be expressed in terms of the expansion coefficients J_i and the area of the fault A. The ISF formation energy γ_{ISF}, where the expansion coefficients up to J_4 are taken into account[1] is

$$\gamma_{ISF} = \frac{4(J_1 + J_2 + J_3 + J_4)}{A} \quad . \quad (2)$$

The expansion coefficients $J's$ used in Eq. 2 are calculated from ordered structures using electronic band structure methods[1],

$$E_{FCC}(N) = J_0 - NJ_1 - NJ_2 - NJ_3 - NJ_4..., \quad (3a)$$

$$E_{HCP}(N) = J_0 + NJ_1 - NJ_2 + NJ_3 - NJ_4..., \quad (3b)$$

$$E_{DHCP}(N) = J_0 + NJ_2 - NJ_4 + ... \quad (3c)$$

Considering up to term J_1 in Eq. 1, reduces the model to its first-order approximation, the axial nearest-neighbor Ising model (ANNI), and γ_{ISF} in this case takes the follwing form[1,25],

$$\gamma_{ISF} = \frac{2E_{HCP} - 2E_{FCC}}{A} \quad . \quad (4)$$

Otherwise, if terms up to J_4 terms are taken into account, the model is reduced to the axial next-nearest-neighbor model (ANNNI) and the double hexagonal close packed (DHCP) structure having the sequence ABACABAC needs to

be considered. Consequently, the γ_{ISF} is now given as[1],

$$\gamma_{ISF} = \frac{E_{HCP} - 3E_{FCC} + 2E_{DHCP}}{A} \quad . \quad (5)$$

In metals, generally, the ANNNI model is sufficient as interactions are generally very short in range[1,18]. The AIM model does not perfectly account for all the effects as the supercell approach does, but it has been found to produce similar results[1,25].

AIM applied to $L1_2$

The (111) SISF formation energy of $L1_2$ compounds can be calculated using the ANNI and ANNNI models using variants of Eqs. 4&5, due to the analogy of stacking sequences between FCC and $L1_2$, HCP and $D0_{19}$, DHCP and $D0_{24}$[1]. Hence, the (111) SISF formation energy of $L1_2$ compounds using the ANNI model becomes,

$$\gamma^{L12}_{ANNI} = \frac{8(E_{D019} - E_{L12})}{V_{L12}^{2/3} \cdot \sqrt{3}} \quad . \quad (6)$$

where V_{L12} is the volume of 4-atoms $L1_2$ unit cell and $V_{L12}^{2/3} \cdot \sqrt{3}$ is the area of 4-atoms in the $L1_2$ (111) plane over which the stacking fault extends. E_{L12} and E_{D019} are the energies per atom of the $L1_2$ and $D0_{19}$ structures.
Similarly, the (111) SISF formation energy of $L1_2$ compounds according to the ANNNI model is,

$$\gamma^{L12}_{ANNNI} = \frac{4\left(E_{D019} - 3E_{L12} + 2E_{D024}\right)}{V_{L12}^{2/3} \cdot \sqrt{3}} \quad . \quad (7)$$

where E_{D024} is the energy per atom of the $D0_{24}$ structure calculated at V_{L12} equilibrium volume.

B. Quasiharmonic Debye Model

In order to get the equation of state EOS, particularly $V = f(T)$, of the different crystalline phases considered here, we employ the quasiharmonic Debye Model[26]. At any given temperature and pressure, the system (crystal phase) is described thermodynamically by the general Gibbs function, denoted as non-equilibrium Gibbs,

$$G^*(T,P,a) \;=\; E_e(a) + PV(a) + A_{vib}(T, w(a))\,. \quad (8)$$

E_e is the total-energy of the system at a lattice parameter a. PV is the constant hydrostatic pressure condition, where P is the pressure and V is the volume. $A_{vib}(T, w(a))$ is the Helmholtz vibrational energy term. The dependence of E_e on the lattice parameter a is explicit, while A_{vib} depends on a, implicitly, through the frequencies of vibration $w(a)$. Since the volume is dependent on a, this gives the desired interdependence between temperature and volume. At a given set of temperature and pressure (T,P), the equilibrium state is the one that minimizes G^* of the crystal phase with respect to volume. The Helmholtz vibrational energy is

$$A_{vib}(T,V) \;=\; U_{vib} - TS_{vib}\,. \quad (9)$$

According to Debye model U_{vib} and S_{vib} are:

$$U_{vib} \;=\; \frac{9}{8} n k_B \Theta_D + 3 n k_B T D(\Theta_D/T)\,, \quad (10)$$

$$S_{vib} \;=\; 4 n k_B D(\Theta_D/T) - 3 n k_B ln\left(1 - e^{-\Theta_D/T}\right)\,, \quad (11)$$

$$D(x) \;=\; \frac{3}{x^3}\int_0^x \frac{\zeta^3 d\zeta}{e^\zeta - 1}\,, \quad (12)$$

$$\zeta \;=\; \frac{hw}{k_B T}\,, \quad (13)$$

$$x \;=\; \frac{\hbar w_D}{k_B T} = \frac{\Theta_D}{T}\,. \quad (14)$$

n is the number of atoms per formula unit and Θ_D is the Debye temperature of the solid which can assume this expression after some assumptions[27],

$$\Theta_D = \frac{\hbar}{k_B} f(\nu) \left(6\pi^2 n V^{1/2}\right)^{\frac{1}{3}} \sqrt{\frac{B_{static}}{M}} \quad (15)$$

M is the molecular mass per formula unit, $\hbar$ is the reduced Planck's constant, k_B is Boltzmann

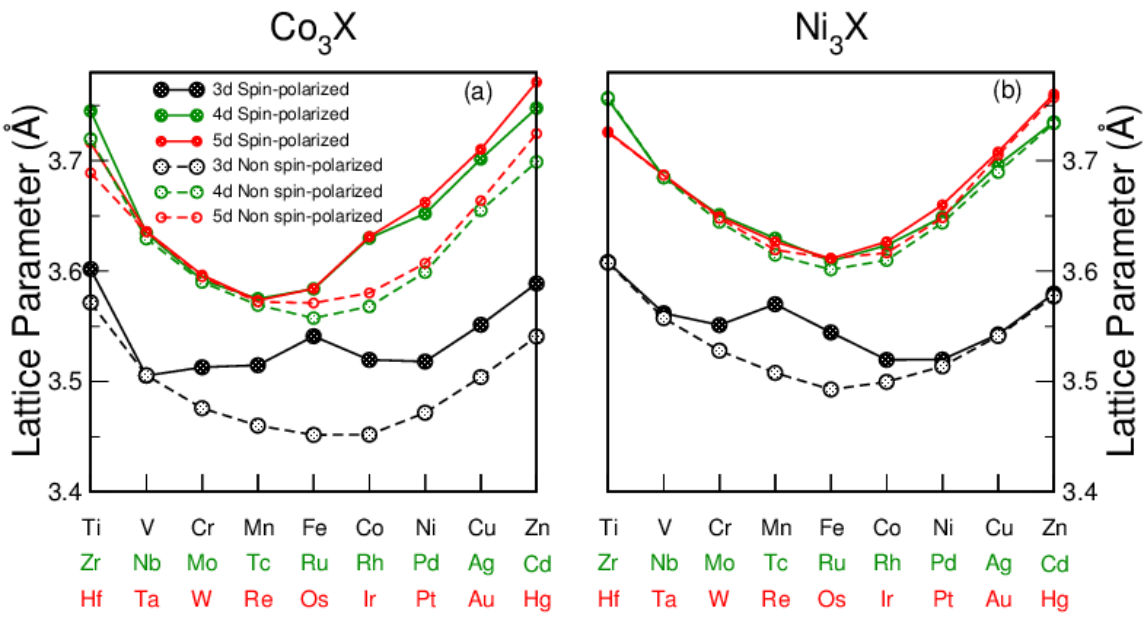

FIG. 1. The change in Co_3X (panel a) and Ni_3X (panel b) 0 K $L1_2$ lattice parameter as a function of X position in the periodic table.

constant, ν is the Poisson ratio of the solid, $f(\nu)$ is given by[27]

$$f(\nu) = \left\{ 3 \left[2 \left(\frac{2}{3} \frac{1+\nu}{1-2\nu} \right)^{3/2} + \left(\frac{1}{3} \frac{1+\nu}{1-\nu} \right)^{3/2} \right]^{-1} \right\}^{1/3} \quad (16)$$

B_{static} the static bulk modulus,

$$B_{static}(V) = V \left(\frac{\partial^2 E_e(V)}{\partial V^2} \right) . \quad (17)$$

Thus the volume dependence of Debye temperature Θ is established. The volume that makes $G^*(T, P; V)$ minimum *i.e*,

$$\left(\frac{\partial G^*}{\partial V} \right)_{T,P} = 0 . \quad (18)$$

is the equilibrium volume for given conditions of T and P, and the set of equilibrium volumes at different temperatures and pressures provides the equation of state (EOS) of solid, $V(T,P)$. The minimization of G^* is implemented in the **gibbs** code[27].

C. First-principles calculations

The calculations reported in this work are based on the density-functional theory[14,15] DFT. The total energies inasmuch they are needed for optimization of the volume were calculated using the projector augmented wave (PAW) method[28] implemented in the Vienna first-principles simulation package (VASP)[29–31]. The exchange correlation energy was treated in the *generalized gradient approximation* (GGA) with the PBE96 functional[32,33]. After necessary tests to control the stability of energy, the energy cut-off was set to 400 eV. A mesh of 165, 192 and 96 special k-points for $L1_2$, $D0_{19}$ and $D0_{24}$, respectively, were taken in the irreducible wedge of the Brillouin zone for the total-energy calculation. The selected number of k-points was determined using the Monkhorst-Pack scheme[34]. We emphasize that convergence tests for the plane-wave cutoff and the number of k-point were essential to assure reliable total-energy differences. The electronic minimisation

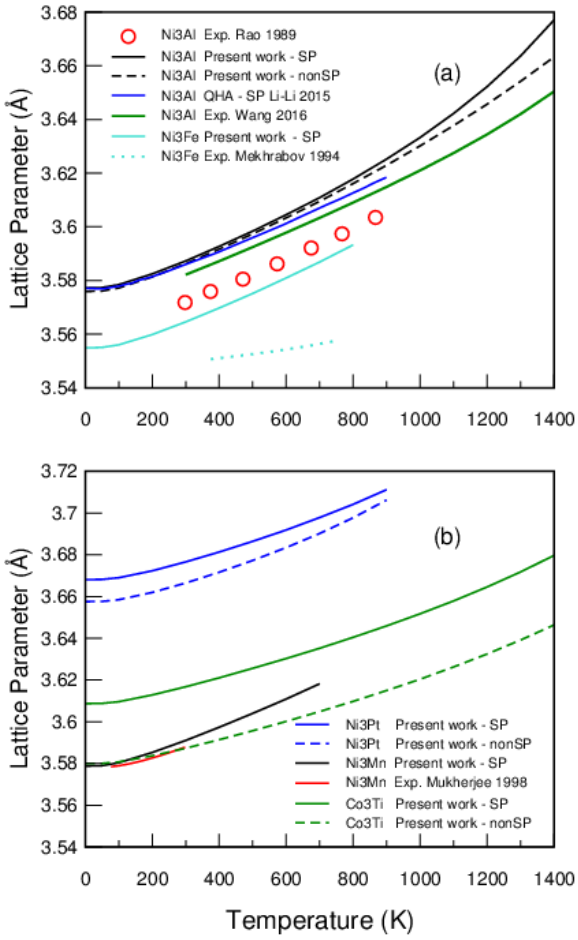

FIG. 2. The variation of the lattice parameters of stable Ni_3X and Co_3X $L1_2$ systems due to thermal expansion. The plotted temperature range of every system corresponds to approximately its critical point (order-disorder phase transition).

was judged complete when the energy difference between steps was less than $1 \cdot 10^{-5}$eV. For 7 elements (Mo, Tc Nb, Rh, Ta, W Os) semi-core states were modelled as valence states using the correspondent potentials.

Regarding the $D0_{19}$ and $D0_{24}$ phases, we emphasize that the total energy was minimized, through performing only local atomic relaxations at the corresponding $L1_2$ equilibrium volume-per-atom and at fixed $D0_{19}$ and $D0_{24}$ ideal c/a ratios, in this way we guaranteed that ($a_{D0_{19}}$ and $c_{D0_{19}}$) and ($a_{D0_{24}}$ and $c_{D0_{24}}$) correspond to the underlying $L1_2$ lattice *i.e.*, ($a_{D0_{19}}/a_{L1_2} = \sqrt{2}$ and $c_{D0_{19}}/a_{L1_2} = \sqrt{4/3}$) and ($a_{D0_{24}}/a_{L1_2} = \sqrt{2}$ and $c_{D0_{24}}/a_{L1_2} = 4/\sqrt{3}$). The atomic positions for both phases were relaxed using the conjugate gradient algorithm[35], a highly recommended scheme to relax the atoms into their instantaneous groundstate, especially in case atomic relaxation is problematic.

III. GROUND STATE PROPERTIES

A. Lattice parameters

The change in the lattice parameter of the $L1_2$ phase in Co_3X and Ni_3X compounds, as a function of X element position in the periodic table, predicted with and without spin-polarized calculations is plotted in Fig. 1. Our lattice constant predictions corresponding to the compounds where $L1_2$ phase has been experimentally evidenced to exist, together with the experimental findings and previous theoretical works, are compared in Table I.

The spin-restricted (non-SP) lattice parameters exhibit an ideal parabolic variation with minimum occuring around the column Fe/Ru/Os. In fact, this minimum at the center of the *d*-band series is attributed to the maximum cohesive energies[51–55] of these half *d*-band filled elements.

Comparatively, the SP lattice parameter variation deviates from the ideal parabolic shape due to magnetism, especially compounds with X belonging to the 3*d* series in general, and X belonging to 4-5*d* series for Co_3X compounds.

It is worth mentioning that our SP lattice parameters are actually very close to the room temperature experimental values, as manifested in Table I. For instance, the difference ranges from 0.03 % for Ni_3Fe to 0.38 % for Ni_3Pt.

We have calculated the lattice parameter temperature-dependence using a quasiharmonic Debye model for the $L1_2$ stable compounds. In Fig. 2(a,b), we present a comparison between

TABLE I. Theoretical (0 K) and room temperature RT experimental lattice parameters of Co_3X and Ni_3X $L1_2$ compounds. The unit is Angstrom (Å).

Compound	Our Calculation (0 K)		Other Calculations (0 K)		Experiments (RT)
	SP	non-SP	Method	Value	
Co_3Ta	3.636	3.635	PAW-GGA-PW91	3.637[4]	3.647[36]
			PAW-GGA	3.64[37]	3.65[37]
					3.67[38]
Co_3Ti	3.602	3.571	PAW-GGA-PW91	3.601[4]	3.612[39]
			LMTO-ASA-LDA	3.58[40]	3.597[41]
Co_3V[a]	3.505	3.505	PAW-GGA-PW91	3.514[4]	—
			LMTO-ASA-LSDA	3.54[42]	
			LMTO-ASA-LDA	3.51[43]	
Ni_3Fe	3.544	3.492	LMTO-ASA-LSDA	3.54[42]	3.545[44]
					3.555[45]
Ni_3Mn	3.57	3.507	LMTO-ASA-LSDA	3.55[42]	3.59[46]
Ni_3Pt	3.66	3.648	PP-PW-GGA-PBE	3.667[47]	3.646[48]
Ni_3Al	3.5689	3.5687			3.5635[49]
					3.5718[50]

[a] Metastable

our work and other theoretical calculations and experimental findings. Let us mention here that the Poisson ratios used in calculating the EOS for the $L1_2$ compounds are 0.4 (Ni_3Al,Ni_3Mn), 0.301 (Ni_3Pt), 0.38 (Ni_3Fe) and 0.39 (Co_3Ti).
Concerning Ni_3Al it is a weak itinerant ferromagnet with very low Curie temperature (T_c=41.5 K) and it retains an ordered structure until it melts (1660 K[56]). Our results are in good agreement with the quasi harmonic phonon calculations[57]. Between RT and 1000 K, the differences between our results and the experimental data are 0.19 %[56] and 0.47 %[50], not very different from the difference between the experimental data themselves (0.26 %). At 1400 K the difference between our data (non-SP) and the experimental data[56] increases to 0.31 %. This relative increase, in spite of its small magnitude, can be explained by the fact that at high temperatures there is a dramatic increment due to anharmonicity which is not accounted for in Debye model. it's worth noting that at high temperatures our SP and non-SP lattice parameters diverge, where the non-SP data are closer to the available experimental data[56]. We find the maximum increase (non-SP) in the lattice parameter due to thermal expansion between RT and 1400 K to be 2 % comparing to 1.88 % experimental increase[56].
Ni_3Fe undergoes a second-order ferromagnetic-to-paramagnetic transition at T_C=870 K and a first-order phase transition from an ordered $L1_2$ to a disordered face centered cubic phase at T_o=780 K. Thus $L1_2$ is ferromagnetic through the whole stable temperature range. Unfortunately, the available experimental data are limited in temperature-range[58]. The agreement between our results and the experiment is less pronounced in comparison with Ni_3Al case, where the difference ranges from 0.46 % (at 375 K) to 0.89 % (at 740 K).
In Ni_3Mn system, atomic ordering to $L1_2$ structure takes place around 753 K accompanied by a ferromagnetic ordering at $T_C \sim 700$ K for a perfectly ordered alloy[59]. Our prediction for the temperature dependence of $L1_2$ Ni_3Mn lattice parameter agrees well (maximum difference is 0.08 %) with the experiment[60] as shown in Fig. 2(b).
The system Ni_3Pt remains ferromagnetic below Tc=373 K[61] and crystallizes in the $L1_2$ structure until about 850 K[62]. On the other hand, Co_3Ti is paramagnetic[63] through whole its temperature stability range ($\sim$ 1400 K[64]). Unfortu-

nately, for these two systems, there is no available experimental data to compare with.

B. Magnetic moment

While few 3*d* elements are ferromagnetic (Fe, Co, Ni), 4*d* and 5*d* elements are all bulk nonferromagnets[71], they are paramagnetic, however, Pd is very close to the Stoner criterion for ferromagnetic ordering but remains only paramagnetic – see Ref. 72 and references therein. As shown in Fig. 4(e & f), many of the 4 and 5*d* elements develop significant local magnetic moments as they occupy the X inequivalent sublattice and all have a strong effect on cobalt or nickel local magnetic moments. However, among the 4-5*d* series only Co_3Ta and Ni_3Pt appear as stable $L1_2$ phases in the phase diagram. Table II shows our 0 K determined magnetic moments, together with calculations from literature and the experimental results. Our predictions are in reasonable agreement with the experiment for the system Ni_3Fe, however we overestimate the local magnetic moment on Ni for the compounds Ni_3Mn, Ni_3Pt, and Ni_3Al, by 30-70%. This is due to the fact that the GGA, as well as *local density approximation* LDA, of the exchange-correlation potential cause the exaggerated increase in the magnetism of these compounds[69,73]

C. Formation enthalpies

A_3B and AB_3 binary compounds can be crystallized in, around, 20 different ordered structures: A15, Ae, $D0_2$, $D0_3$, $D0_9$, $D0_{11}$, $D0_{18}$, $D0_{19}$, $D0_{20}$, $D0_{21}$, $D0_{22}$, $D0_{23}$, $D0_{24}$, $D0_a$, $D0_b$, $D0_c$, $D0_d$, $L1_2$, $L1_a$, and $L6_0$. $L1_2$ and $D0_{19}$ are the most simple ones in comparison to the other structures as they have small number of atoms per unit cell. They can be easily formed, as metastable phases, in non-equilibrium processing techniques (solid-state interfacial reaction or ion beam mixing) in contrast to the other relatively larger complicated structures. In fact, even if the formation of some of these complicated structures are thermodynamically favorable *i.e.*, they are characterized by low formation enthalpies relative to the other structures, their experimental observation is not straight forward, since they need long high-temperature treatment to improve the atomic mobility in order for the atoms to arrange themselves into an ordered configuration[80].

In this study we are concerned with the formation enthalpies exclusively of the $L1_2$ phase for Co_3X and Ni_3X compounds. The enthalpies of formation ΔH of Co_3X compounds were calculated using

$$\Delta H_{L1_2}^{Co_3X} = E_{L1_2}^{Co_3X} - \frac{3}{4}E_{hcp}^{Co} - \frac{1}{4}E_{\phi}^{X}, \quad (19)$$

and those of Ni_3X compounds,

$$\Delta H_{L1_2}^{Ni_3X} = E_{L1_2}^{Ni_3X} - \frac{3}{4}E_{fcc}^{Ni} - \frac{1}{4}E_{\phi}^{X}. \quad (20)$$

where E_{ϕ}^{X} is the total energy of the X element in its ground state structure ϕ.

As shown in Fig. 4, the compounds that appear to be $L1_2$ phase-forming ones are: Co_3(X=Ti,Zr,Hf,V,Nb,Ta,W,Pt) and Ni_3(X=Ti,Zr,Hf,V,Nb,Ta,Cr,Mn,Fe,Zn,Pt), as they have negative formation enthalpies. However, in the absence of the enthalpies of the aforementioned competent ordered phases and the random solid solutions, the negative sign here is not enough to make these compounds stable *i.e.*, to appear on the phase diagram. Our purpose from plotting the $L1_2$ enthalpies as a function of the X position in the periodic table is to check a possible dependence of the enthalpy on the *d*-band filling. Indeed, we find the 3*d* (non-SP calculations) and 4-5*d* band series to manifest a clear dependence on the X position, where X situated to the left of the column Cr/Mo/W results in negative enthalpies, while X to the right produces positive values, Pt and Zn stand out as an exception to this observation. Furthermore to be noted, SP calculation of the 3*d* series changes substantially the enthalpies, making $L1_2$ Ni_3Mn and Ni_3Fe phase-forming, also Ni_3Cr albeit has small negative enthalpy (-0.3 KJ/mol.atom).

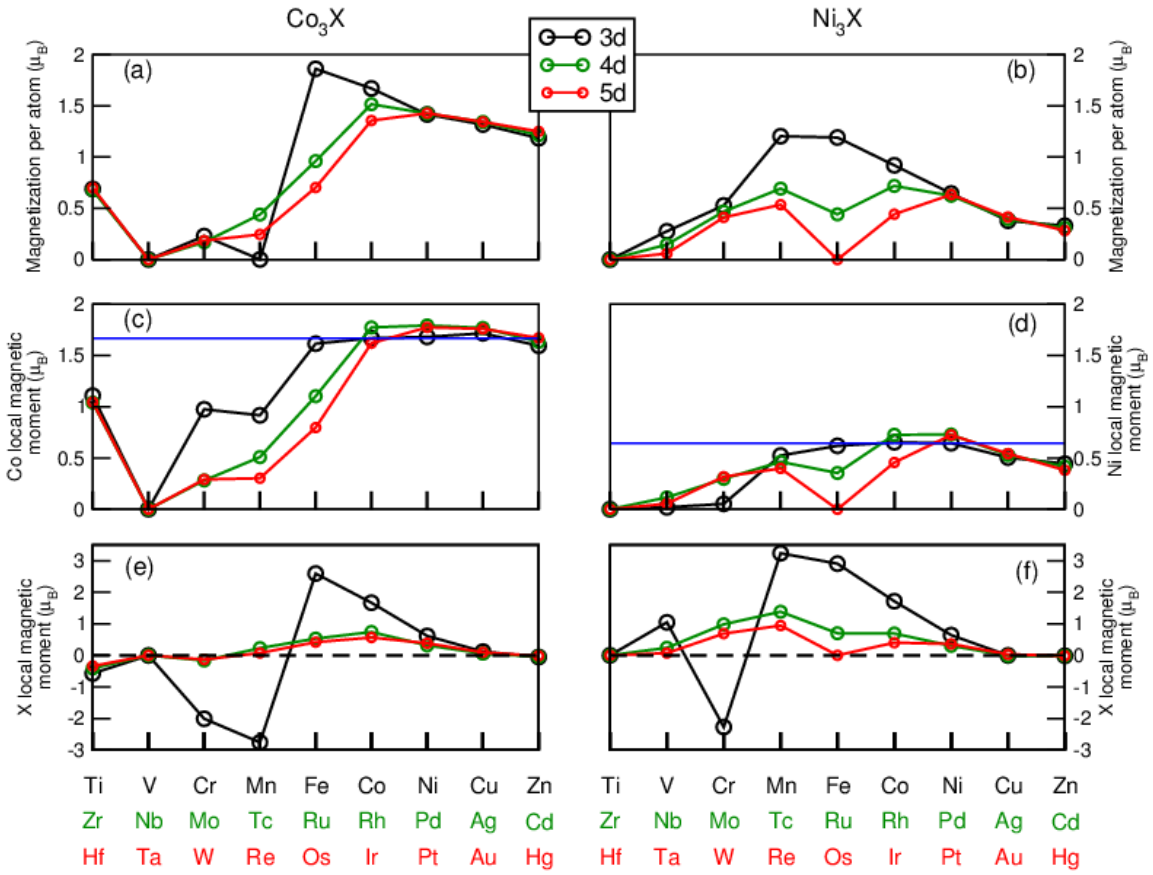

FIG. 3. (a,b) Total magnetization per atom, (c,d) Co/Ni local magnetic moment, and (e,f) local magnetic moment on the element X, in Co_3X and Ni_3X compounds. The blue solid line in panels (c) and (d) designates the local magnetic moment on Co and Ni in the fcc structure, respectively.

TABLE II. Theoretical and experimental total magnetization (per atom) and local magnetic moment on Co, Ni and X element, in Bohr magneton (μ_B), for experimentally observed Co_3X and Ni_3X $L1_2$ phases.

	Our calculation			Other Calculations			Experiments		
Compound	Tot	Co/Ni	X	Tot	Co/Ni	X	Tot	Co/Ni	X
Co_3Ti	0.6875	1.1077	−0.572	—	—	—	—	—	—
Ni_3Fe	1.1905	0.6183	2.906	1.23[65a]	0.66[65]	2.94[65]	1.2075[66]	0.62[66]	2.97[66]
Ni_3Mn	1.2025	0.5247	3.236	1.25[65b]	0.57[65]	3.31[65]	1.02[66]	0.30[66]	3.18[66]
Ni_3Pt	0.6335	0.7245	0.3625	0.60[67c]	—	—	0.424[68†]	0.48[68†]	0.254[68†]
Ni_3Al	0.19	0.256	−0.008	0.236[69d]	—	—	0.0575[70]	0.077[70]	—

[†] interpolated values

[a] FLAPW-GGA-PBE
[b] FLAPW-GGA-PBE
[c] PAW-GGA-PBE
[d] FLAPW-LDA

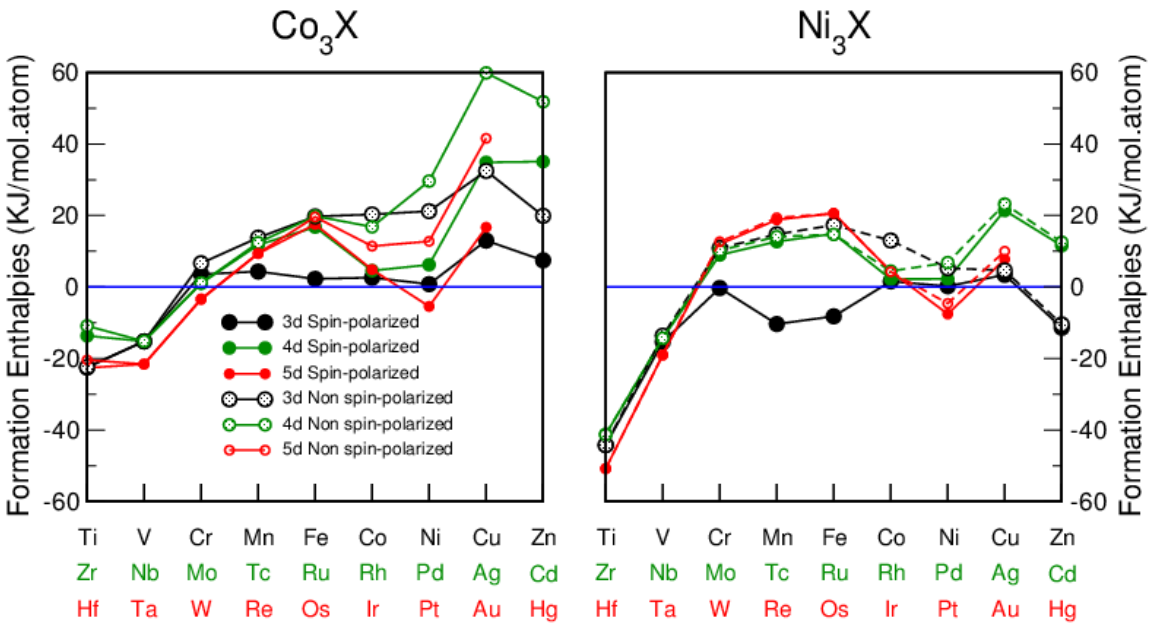

FIG. 4. 0 K formation enthalpies of $L1_2$ phase in (a) Co_3X and (b) Ni_3X compounds

Experimentally, the $L1_2$ phase has been observed only in these compounds: Co_3X(X=Ti[39,41,75],Ta[36,37]) and Ni_3X(X=Mn[77],Fe[44,45],Pt[48]). It is worth mentioning that Ref. 67 has shown that $L1_2$ phase of Ni_3Pt is not the most stable phase at 0 K, though it is stabilized around 413 K due to vibrational entropy. Within the same context, let us note that the Co_3V $L1_2$ ordered-phase was observed in the quenched alloys with a composition around 25 at.%V[81–83], moreover, Refs. 81 and 82 claimed that there is a single $L1_2$ ordered-phase region between (αCo) and Co_3V phase. Nevertheless, the phase with $L1_2$ ordered-structure was confirmed to be metastable, and the formation of $L1_2$ ordered-phase was probably caused by quenching[84].
The fact that the lowest formation enthalpies of Co_3X compounds correspond to X element belonging to Ti/Zr/Hf and V/Nb/Ta columns and the fact that these elements, except V, strongly partition to the W sublattice[85] in a $L1_2$ Co_3(W,X) alloy, indicate that these elements, with fine-tuning of their compositions, can enhance the low stability of the extremely important $L1_2$ Co_3(Al,W) alloy[86,87]. Indeed, Ref. 88 has shown that a small additions of Hf stabilizes the $L1_2$ at a composition around $Co_{0.772}Al_{0.102}W_{0.123}Hf_{0.003}$. Ref. 8 has aslo shown that Ti and Ta additions are found to strongly partition to the γ' phase and greatly increase its volume fraction.

$L1_2$ Ni_3Zn

It is interesting to point out to the low formation enthalpy (−11.5 KJ/mol.atom) of the $L1_2$ Ni_3Zn phase, using SP and non-SP schemes. This phase is not known to appear in the actual Ni-Zn phase diagram[89]. The solubility range of Zn in Ni ranges from $\sim$ 23 at.% Zn at $\sim$ 250 K to $\sim$ 37 at.% Zn at $\sim$ 1250 K[89]. The stable phase is fcc solid solution (α phase). The experimental formation enthalpy of the α phase at the composition 25 at.% Zn is −8.5 KJ/mol.atom measured at 1100 K[89]. In order to investigate this issue, we perform calculations to de-

TABLE III. Theoretical (0 K) and experimental formation enthalpies of $L1_2$ phase in Co_3X and Ni_3X compounds. The unit is KJ/mol.atom.

Compound	Our Calculation (0 K)		Other Calculations (0 K)		Experiments
	SP	non-SP	Method	Value	
Co_3Ta	−21.56	−21.56	PAW-GGA	−30.875[37]	—
			PAW-GGA-PBE	−22[74]	
			PAW-GGA-PW91	−24.844[4]	
Co_3Ti	−22.51	−22.51	PAW-GGA-PW91	−25.843[4]	−26.18[75] (298 K)
			LMTO-ASA-LDA	−26.5[40]	
			PAW-GGA-PBE	−24.9[74]	
Co_3V[a]	−15.20	−15.20	PAW-GGA-PW91	−18.38[4]	—
Ni_3Fe	−8.2	17.32	FLAPW-GGA-PW91	−8.65[76]	—
Ni_3Mn	−10.35	14.74	—	—	−7.93[77b]
Ni_3Pt	−7.54	−4.6	PAW-LDA	−6.31[78]	—
Ni_3Al	−42.1	−41.8	PAW-GGA	−41.1[79] (300K)	−47[79] (300K)
					−41.31[79] (300K)
					−40.59[79] (300K)
					−38.24[79] (300K)

[a] Metastable
[b] Corresponds to 76.2 at. % Ni

termine the formation enthalpy of the fcc random solid solution alloy at the composition 25 at.% Zn. The alloy was modeled by constructing two different supercells: the first of 32 atoms $2\times2\times2(\times4$-atoms) and the second of 256 atoms $4\times4\times4(\times4$-atoms). To get a random distribution of atoms we minimize the Warren-Cowley short-range order (SRO) parameters[90,91] at several nearest neighbor coordination shells. We employ a calculating set-up identical to that used in $L1_2$ Ni_3Zn *i.e,* same energy cut-off (400 eV) and high number of k-points. Restricting the relaxation to the supercells volume gives -8.56 KJ/mol.atom for the 32-atom supercell and −8.853 KJ/mol.atom for the 256-atom supercell. Allowing local atomic relaxations for the 32-atom supercell reduces the formation enthalpy to −10.62 KJ/mol.atom. Hence, the formation enthalpy of the ordered $L1_2$ phase is still lower than the disordered fcc phase by ~ 1 KJ/mol.atom. In fact, even if the $L1_2$ phase has a lower formation enthalpy than the α phase, that does not automatically mean it can be observed at low temperature (if there are no kinetic restrictions). In principle, one needs to study the Helmholtz energy difference ΔF between the two phases as a function of temperature. This includes the enthalpy and Helmholtz energy due to thermal vibrations (phonons) and to thermally excited electrons. The Helmholtz energy of the fcc phase has an additional configurational entropy term due to atomic disorder to be considered.

IV. SISF ENERGIES

Depending on the stability and energies of the APB, CSF and SISF in the octahedral slip plane in $L1_2$ alloys, the superdislocation can assume this configuration: dissocciation into two super Shockley partials bounded by a SISF, known as SISF-type or type-II dissocciation

$$\langle\bar{1}10\rangle \longrightarrow \frac{1}{3}\langle121\rangle + \text{SISF} + \frac{1}{3}\langle21\bar{1}\rangle\,. \quad (21)$$

In fact Paidar *et al.*[100], within the frame of the linear theory of elasticity of an isotropic continuum, proposed that SISF-type dissocciation (Eq. 21) occurs if the following condition is sat-

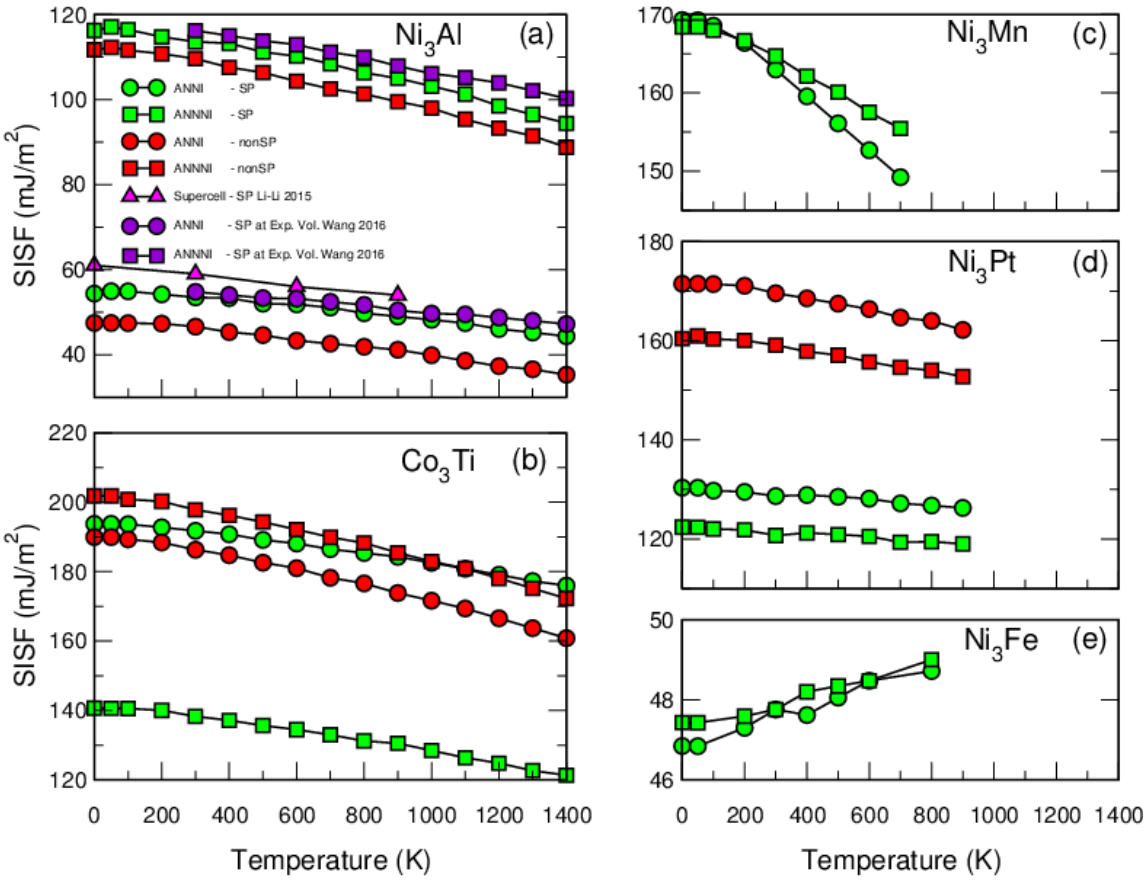

FIG. 5. SISF energies on the (111) plane of stable Co_3X and Ni_3X $L1_2$ compounds variation as a function of temperature. The curves of different compounds are delimited to the stability temperature of the ordered $L1_2$ phase.

isfied – written conveniently as[93,101]

$$\ln\left(\frac{8\pi\gamma_{SISF}^{111}}{C_{44}a_0}\right) < 2\ln\left(\frac{4\pi\gamma_{APB}^{111}}{C_{44}a_0}\right) + 1 \quad (22)$$

$$\delta < 2\pi eC \quad . \quad (23)$$

where the defect energy ratio $\delta = \gamma_{SISF}^{111}/\gamma_{APB}^{111}$ and $C = \gamma_{APB}^{111}/(C_{44}a_0)$ are dimensionless quantities; a_0 is $L1_2$ lattice parameter. γ_{SISF}^{111} and γ_{APB}^{111} are the SISF and APB formation energies on the (111) plane, respectively. Eq. (23) gives the condition for an (111) APB instability with respect to the formation of an (111) SISF.

According to the condition present above (Eq. 23), the knowledge of (111) SISF energies are of extreme importance to judge whether SISF-type dissociation would take place. As a matter of fact, a special type of deformation behaviour has been observed, particularly at low temperatures in some materials: a dramatic increase of flow stress with decreasing temperature. This behaviour is characterstic of compounds and alloys having low SISF energies, favouring thus the dissociation into two super Shockley partials bounded by a SISF. For instance, the plastic flow of Co_3Ti single crystals[102] at low temperatures (< 500 K) is due

TABLE IV. A comparison of the SISF formation energies for the stable Co_3X and Ni_3X $L1_2$ compounds between our work (0 K), other theoretical investigations done with supercell method (0 K), and available experimental data. The unit is mJ/m^2.

Compound	Our Calculation (0 K)				Other Calculations (0 K)		Experiments
	ANNNI		ANNI		Method	Value	
	SP	non-SP	SP	non-SP	—	—	—
Co_3Ti	144	208	197	196	TB-LMTO	175[92]	—
					PP-PAW	210[93]	—
Ni_3Fe	29	5	34	15	—	—	—
Ni_3Mn	165	-194	169	-204	—	—	—
Ni_3Pt	119	162	128	173	—	—	—
Ni_3Al	117	114	55	49	TB-LMTO	147[92]	5-15[94] (623 K)
					FLAPW	40[95]	6±0.5[13] (673 K)[a]
					FP-LMTO	60[96]	
					Empirical Potential	11[97]	
					PP-PAW	43[93]	
					FP-LMTO	80[98]	
					PP-PAW	66.81[99]	

[a] The prepared alloy is non-stoichiometric: $Ni_{0.78}Al_{0.22}$.

to the dislocation movement of the superpartials dissocciated on the (111) plane bounded by a SISF.

We have calculated the (111) SISF energies of the $L1_2$ phase for the compounds where $L1_2$ is stable. The calculation was done by employing the ANNI and ANNNI models, described earlier in section II A, and using the spin-polarized and spin-restricted schemes. We present in table IV a comparison between our results, other theoretical work, and the available experimental data. It seems that there are very few experimental efforts to determine the different planar fault energies in general and none to determine the (111) SISF energies for the compounds considered in this study, apart from Ni_3Al compound, of course. Let us note once more that the transmision electron microscopy technique used to determine the planar fault energies is known to involve incorrect assumptions, and consequently produces sometimes inaccurate values, particularly for the superlattice intrinsic stacking fault energies – see Ref. 103 and references therein. Furthermore, the experimental determination of fault energies depends heavily on the type of elasticity theory applied. Our predictions agree with some theoretical reports and disagree with some others. This is due to the fact that the different reported data on SISF are calculated with different *ab initio* methods, as well as different methodologies to get the SISF energies (supercell vs. AIM). Concerning Co_3Ti compound, we find the (111) SISF formation energy, calculated using the SP and nonSP ANNI model, to be 197 and 196 mJ/m^2 respectively, close to the value reported by Ref. 92 and 93. The low (111) SISF value relative to the high (001) and (111) APB experimental[104] energies 210 and 270 mJ/m^2 respectively, and relative to the theoretical[92] energies 280 and 301 mJ/m^2 respectively, explains the increase in the flow stress with decreasing temperature in this compound[105]. In fact, low SISF (relative to ABP energies) leads to sessile SISF dissocciated superdislocations[105,106]. Furthermore, the difference between SP and non-SP calculations of the SISF formation energy for Ni_3Mn, shows the importance of magnetism in determining correctly the SISF fault in this compound. An improper treatment of this compound discounting magnetism produces negative SISF formation energy. This observation is in contrast to the other presently studied magnetic compounds, where both SP and non-SP

calculations yield different values but same sign. Theoretical investigations of the temperature dependence of SISF energies for $L1_2$ Co_3X and Ni_3X are almost absent in the literature. Hence, we find it necessary to study the SISF energies change as a function of temperature. To this end, we use a quasistatic approach to calculate SISF temperature dependence. It is based on the assumption that the change in SISF upon temperature increase is solely caused by thermal expansion. This approach has been successfully used to calculate the elastic constants of Ni_3Al[107,108]. There are plentiful experimental evidences[109–111] supporting this approximation. It has been as well successfully used to calculate SISF energies in unaries[112] and alloys[113] characterized by complex magnetic structures.
The SISF temperature dependence was established using Eqs. 6&7, by determining the energies of $L1_2$, $D0_{19}$ and $D0_{24}$ phases at $L1_2$ equilibrium volume V corresponding to a temperature T. The volume temperature-dependence $V(T)$ was already established in section III A. As shown in Fig. 5, the tendency of SISF, using both approximations of the AIM model, is to decrease with temperature for the all compounds except for Ni_3Fe where it shows a small increase. The overall decrease in SISF as a function of temperature is $\sim$ 20 % (Ni_3Al), $\sim$ 15 % (Co_3Ti), $\sim$ 12 % (Ni_3Mn), $\sim$ 4 % (Ni_3Pt). All the compounds don not exhibit a sharp or abrupt decrease towards zero . This is understood since according to the relevant phase diagrams, the present $L1_2$ compounds either undergo a phase transition to fcc random phase or remain stable and ordered until melting such as Ni_3Al and Co_3Ti, but not to an hcp-like phase. Note that there is a small difference between the 0 K results in Table IV and their counterparts in Fig. 5, which is attributed to the zero point thermal expansion.
The increase in SISF for the system Ni3Fe can not be related to its ferromagnetic nature since also Ni3Mn is ferromagnetic yet the SISF energy decreases with temperature. The SISF increase in Ni3Fe is purely related to thermal expansion. As the volume increases due to temperature, the presence of Fe on the second sublattice increases the stability of $L1_2$ lattice with respect to hexagonal close packed like-environment, thus SISF increases. This senario is not similar when Al, Mn and Pt, occupy the second sublattice, where a thermaly epanded volume results in decreasing the 0 K SISF value. The increasingly expanded volume improves the bonding energy between Ni and Fe in the $L1_2$ structure in comparison with that in $D0_{19}$, while it lowers the bonding energy between Ni and Mn, also between Ni and Al.
For the system Ni_3Al (Fig. 5(a)), our SP ANNI results are in accordance with the SP quasiharmonic phonon supercell method values[57], while the SP ANNNI results greatly disagree. We have as well calculated the SISF at the experimental volumes[56], this technique has shown to produce values close to the experiment[113]. Unfortunately, there is no experimental data to compare with. The only available experimental values are 5-15[94] mJ/m^2 (623 K) and 6 ± 0.5[13] mJ/m^2 (673 K), and they are closer to the nonSP ANNI results.
On the other hand, there is a significant difference between ANNI and ANNNI results for the systems Ni_3Al and Co_3Ti, which persists with temperature. This can not be related to magnetism, as the difference is also present, in Ni_3Al compound, between nonSP ANNI and ANNNI approximations. Considering the fact that the ANNI results of Ni_3Al are closer to a completely different theoretical approach[57] and relatively closer to the available experimental data[13,94], we suggest that the current implementation[23] of the AIM model restricted to pair interaction is not sufficient to reproduce the supercell method values, at least for some systems, and thus a triple interaction implementation is necessary to converge the AIM to the supercell results.

V. CONCLUSIONS

We have performed first-principles calculations for the $L1_2$ phase in Co_3X and Ni_3X compounds. We find the studied properties of several compounds to show a strong dependence on

magnetism. The different addressed properties show a systematic dependence on the X element position in the periodic table. Our results suggest that the elements Ti, Zr, Hf, Nb and Ta are potential stabilizers for the $Co_3Al_{0.5}W_{0.5}$ alloy. First-principles calculations are highly encouraged to be performed on $Co_3Al_{0.5-x}W_{0.5-x}X_{2x}$ alloy at a single low compostion x in order to test this hypothesis. Our simulation sheds light on the small energetic difference between the ordered $L1_2$ and the disordered fcc phase of Ni-25 at.%Zn alloy.

ACKNOWLEDGMENTS

This work used the ARCHER UK National Supercomputing Service (http://www.archer.ac.uk), University of Birmingham's BlueBEAR HPC service (http://www.birmingham.ac.uk/bear), and computing resources through the MidPlus Regional HPC Centre, we therefore would like to acknowledge them. Also, we would like to acknowledge the EPSRC (grant EP/M021874/1) and EU FP7 (grant GA109937) for financial support.

* corresponding author; a.breidi@hotmail.com

[1] A. Mottura, A. Janotti, and T. M. Pollock. *Intermetallics*, 28:138–143, 2012. doi: 10.1016/j.intermet.2012.04.020. URL `http://dx.doi.org/10.1016/j.intermet.2012.04.020`.

[2] J. R. Davis. *Heat-Resistant Materials*, volume 113. ASM International, Almere, Netherlands, 1997.

[3] Y. M. Eggeler, M. S. Titus, A. Suzuki, and T. M. Pollock. *Acta Materialia*, 77:352–359, 2014. doi: 10.1016/j.actamat.2014.04.037. URL `http://dx.doi.org/10.1016/j.actamat.2014.04.037`.

[4] W. W. Xu, J. J. Han, Z. W. Wang, C. P. Wang, Y. H. Wen, X. J. Liua, and Z. Z. Zhu. *Intermetallics*, 32:303–311, 2013. doi: 10.1016/j.intermet.2012.08.022.

[5] A. Suzuki and T. M. Pollock. *Acta Materialia*, 56:1288–1297, 2008. doi: 10.1016/j.actamat.2007.11.014.

[6] C. T. Sims. *Superalloys 1984*. The Minerals, Metals and Materials Society , Glassport, Pennsylvania, United States, 1984. doi: 10.7449/1984/Superalloys{_}1984{_}399{_}419.

[7] D. Hull and D. J. Bacon. *Introduction to Dislocations*. Elsevier, Amsterdam, Netherlands, 5 edition, 2011. ISBN 978-0-08-096672-4.

[8] I. Povstugar, P. P. Choi, S. Neumeier, A. Bauer, C. H. Zenk, M. Göken, and D. Raabe. *Acta Materialia*, 78:78–85, 2014. doi: 10.1016/j.actamat.2014.06.020.

[9] J. Sato, T. Omori, K. Oikawa, I. Ohnuma, R. Kainuma, and K. Ishida. *Science*, 312:90–91, 2006. doi: 10.1126/science.1121738.

[10] M. S. Titus, A. Mottura, G. B. Viswanathan, A. Suzuki, M. J. Mills, and T. M. Pollock. *Acta Materialia*, 89:423–437, 2015. ISSN 13596454. doi: 10.1016/j.actamat.2015.01.050. URL `http://dx.doi.org/10.1016/j.actamat.2015.01.050`.

[11] N. L. Okamoto, T. Oohashi, H. Adachi, K. Kishida, H. Inui, and V. Patrick. *Philosophical Magazine*, 91:3667–3684, 2011. doi: 10.1080/14786435.2011.586158.

[12] A. Bauer, S. Neumeier, F. Pyczak, and M. Göken. *Scripta Materialia*, 63:1197–1200, 2010. doi: 10.1016/j.scriptamat.2010.08.036.

[13] H. P. Karnthaler, E. TH. Mühlbacher, and C. Rentenberger. *Acta Materialia*, 44(2):547–560, 1996. doi: 10.1016/1359-6454(95)00191-3.

[14] P. Hohenberg and W. Kohn. *Phys. Rev.*, 136:B864–B871, Nov 1964. doi: 10.1103/PhysRev.136.B864. URL `http://link.aps.org/doi/10.1103/PhysRev.136.B864`.

[15] W. Kohn and L. J. Sham. *Phys. Rev.*, 140:A1133–A1138, Nov 1965. doi: 10.1103/PhysRev.140.A1133. URL `http://link.aps.org/doi/10.1103/PhysRev.140.A1133`.

[16] G. Schoeck, S. Kohlhammer, and M. Fahnle. *Philosophical Magazine Letters*, 79:849–857, 1999. doi: 10.1080/095008399176544.

[17] M. Chandran and S. K. Sondhi. *Journal of Applied Physics*, 109:1–6, 2011. doi: 10.1063/1.3585786.

[18] L. Vitos, J. O. Nilsson, and B. Johansson. *Acta Materialia*, 54:3821–3826, 2006. doi: 10.1016/j.actamat.2006.04.013.

[19] Y. Qi and R. K. Mishra. *Physical Review B*, 75:224105, 2007. doi: 10.1103/PhysRevB.75.224105. URL `http://link.aps.org/doi/10.1103/PhysRevB.75.224105`.

[20] Kenneth A. Green, Tresa M. Pollock, and Robert D. Kissinger. *Superalloys 2000*. The Minerals, Metals and Materials Society , Glassport, Pennsylvania, United States, 2000.

[21] J. Hafner. *Computer Physics Communications*, 177:6–13, 2007. doi: 10.1016/j.cpc.2007.02.045.

[22] J. Yan, C. Wang, and S. Wang. *Physical Review B*, 70:174105–174110, 2004. doi: 10.1103/PhysRevB.70.174105.

[23] P J H Denteneer and W van Haeringen. *Journal of Physics C: Solid State Physics*, 20(32):L883, 1987. URL `http://stacks.iop.org/0022-3719/20/i=32/a=001`.

[24] K. Ishida. *Physica Status Solidi (a)*, 36:717–728, 1976.

[25] A. Dick, T. Hickel, and J. Neugebauer. *Steel Research International*, 80:603–608, 2009. doi: 10.2374/SRI09SP015. URL `http://onlinelibrary.wiley.com/doi/10.2374/SRI09SP015/abstract`.

[26] Alexei A Maradudin. *Theory of lattice dynamics in the harmonic approximation*. New York,Academic Press, 1963. doi: http://hdl.handle.net/2027/mdp.39076006406289.

[27] M.A. Blanco, E. Francisco, and V. Luaña. *Computer Physics Communications*, 158 (1):57 – 72, 2004. doi: http://dx.doi.org/10.1016/j.comphy.2003.12.001. URL `http://www.sciencedirect.com/science/article/pii/S0010465503005472`.

[28] P. E. Blöchl. *Phys. Rev. B*, 50:17953–17979, Dec 1994. doi: 10.1103/PhysRevB.50.17953. URL `http://link.aps.org/doi/10.1103/PhysRevB.50.17953`.

[29] G. Kresse and J. Hafner. *Phys. Rev. B*, 47:558–561, Jan 1993. doi: 10.1103/PhysRevB.47.558.

[30] G. Kresse and J. Hafner. *Phys. Rev. B*, 49:14251–14269, May 1994. doi: 10.1103/PhysRevB.49.14251.

[31] G. Kresse and J. Furthmüller. *Computational Materials Science*, 6(1):15 – 50, 1996. doi: http://dx.doi.org/10.1016/0927-0256(96)00008-0.

[32] John P. Perdew, Kieron Burke, and Matthias Ernzerhof. *Phys. Rev. Lett.*, 77:3865–3868, Oct 1996. doi: 10.1103/PhysRevLett.77.3865. URL `http://link.aps.org/doi/10.1103/PhysRevLett.77.3865`.

[33] J. P. Perdew, K. Burke, and M. Ernzerhof. *Physical Review Letters*, 78(7):1396, 1997. doi: 10.1103/PhysRevLett.78.1396.

[34] J. D. Pack and H. J. Monkhorst. *Physical Review B*, 16(4):1748–1749, 1977. doi: 10.1103/PhysRevB.16.1748.

[35] W.H. Press, S.A. Teukolsky, W.T. Vetterling, and B.P. Flannery. Cambridge University Press, 2007. ISBN 9780521880688. URL `http://books.google.fr/books?id=1aAOdzK3FegC`.

[36] R. D. Dragsdorf. *Acta Cryst*, 15:531–536, 1962. doi: 10.1107/S0365110X62001371.

[37] Xiang He, Ling-Ti Kong, and Bai-Xin Liu. *Journal of the Physical Society of Japan*, 74:2501 – 2505, 2005. doi: 10.1143/JPSJ.74.2501.

[38] V.V. Peťkov, Y.A. Kocherzhinskii, and V.Y. Markiv. *Dopov. Akad. Nauk Ukr. RSR, Ser. A*, pages 852–854, 1971.

[39] A. K. Sinha. *Trans.AIME*, 245:911, 1969.

[40] J. Xu and W. Lin. *Physical Review B*, 48(7):4276–4286, 1993.

[41] F. Cruz-Gandarilla, R. Gayosso-Armenta, M. Hesquio-Gardu no, J. G. Caba nas Moreno, and R. Martínez-Sánchez. *Materials Science Forum*, 442:109–114, 2003. doi: 10.4028/www.scientific.net/MSF.442.109.

[42] Y. Tanaka, S. Ishida, and S. Asano. *Materials Transactions*, 46(2):355–360, 2005.

[43] J. Xu and A. J. Freeman. *Physical Review B*, 45(19):863–871, 1992.

[44] M. King, W. F. McClune, L. C. Andrews, M. A. Holomany, T. M. Kahmer, B. Lawyer, L. Zwell, B. Post, S. Weissmann, H. F. McMrdie, P. Bayliss, and M. E. Mrose. *Mineral Powder Diffraction File Databook: Sets 1-42*. JCPDS-International Centre for Diffraction Date 1601 Park Lane, Swarthmore, Pennsylvania 19081-2389U.S.A, 1993.

[45] A. Lutts and P. M. Gielen. *physica status solidi (b)*, 41(1):K81–K84, 1970. doi: 10.1002/pssb.19700410169.

[46] E. A. Brandes and G. B. Brook, editors. *Smithells Metals Reference Book*. Butterworth-Heinemann, London, UK, 7th edition, 1992.

[47] Q. Chen, Z. Huang, Z. Zhao, and C. Hu. *Applied Physics A*, 116:1161–1172, 2014. doi: 10.1007/s00339-013-8201-6.

[48] A. Pisanty, C. Amador, Y. Ruiz, and M. de la Vega. *Zeitschrift für Physik B Condensed Matter*, 80(2):237–239, 1990. doi: 10.1007/BF01357508. URL http://dx.doi.org/10.1007/BF01357508.

[49] K. Aoki, , and O. Izumi. *physica status solidi (a)*, 32(2):657–664, 1975. doi: 10.1002/pssa.2210320240. URL http://dx.doi.org/10.1002/pssa.2210320240.

[50] P V Mohan Rao, S V Suryanarayana, K Satyanarayana Murthy, and S V Nagender Naidu. *Journal of Physics: Condensed Matter*, 1(32):5357, 1989. URL http://stacks.iop.org/0953-8984/1/i=32/a=004.

[51] A. Breidi, S. G. Fries, and A. V. Ruban. *Phys. Rev. B*, 93:144106, Apr 2016. doi: 10.1103/PhysRevB.93.144106. URL http://link.aps.org/doi/10.1103/PhysRevB.93.144106.

[52] M. Cyrot and F. Cyrot-Lackmann. *Journal of Physics F: Metal Physics*, 6(12):2257, 1976. URL http://stacks.iop.org/0305-4608/6/i=12/a=012.

[53] F. Cyrot-Lackmann. *Journal of Physics and Chemistry of Solids*, 29(7):1235 – 1243, 1968. doi: http://dx.doi.org/10.1016/0022-3697(68)90216-3.

[54] J. Friedel. In J. M. Ziman, editor, *Physics of Metals*. Cambridge University Press, New York, 1969.

[55] D.G. Pettifor. *solid State Physics*, 40:43 – 92, 1987. doi: http://dx.doi.org/10.1016/S0081-1947(08)60690-6. URL http://www.sciencedirect.com/science/article/pii/S0081194708606906.

[56] Hai-Peng Wang, Peng Lü, Kai Zhou, and Bing-Bo Wei. *Chinese Physics Letters*, 33(4):046502, 2016. URL http://stacks.iop.org/0256-307X/33/i=4/a=046502.

[57] Liu Li-Li, Wu Xiao-Zhi, Wang Rui, Li Wei-Guo, and Liu Qing. *Chinese Physics B*, 24(7):077102, 2015. URL http://stacks.iop.org/1674-1056/24/i=7/a=077102.

[58] A. O. Mekhrabov. *Acta Physica Polonica A*, 85:571, 1994.

[59] N. Thompson. *Proc. Phys. Soc.*, 52:217, 1940.

[60] Goutam Dev Mukherjee, C. Bansal, and Ashok Chatterjee. *International Journal of Modern Physics B*, 12(22):2233–2246, 1998. doi: 10.1142/S0217979298001307. URL http://www.worldscientific.com/doi/abs/10.1142/S0217979298001307.

[61] P. Nash and MF Singleton. *Bull Alloy Phase Diagrams*, 10:258, 1989.

[62] Xiao-Gang Lu, Bo Sundman, and John Ågren. *Calphad*, 33(3):450 – 456, 2009. doi: http://dx.doi.org/10.1016/j.calphad.2009.06.002. URL http://www.sciencedirect.com/science/article/pii/S0364591609000492.

[63] Y. Aoki. *Journal of the Physical Society of Japan*, 28(6):1451–1456, 1970. doi: 10.1143/JPSJ.28.1451. URL http://dx.doi.org/10.1143/JPSJ.28.1451.

[64] A. V. Davydov, U. R. Kattner, D. Josell, R. M. Waterstrat, W. J. Boettinger, J. E. Blendell, and A. J. Shapiro. *Metallurgical and Materials Transactions A*, 32(9):2175–2186, 2001. doi: 10.1007/s11661-001-0193-8. URL http://dx.doi.org/10.1007/s11661-001-0193-8.

[65] S.E Kulkova, D.V Valujsky, Jai Sam Kim, Geunsik Lee, and Y.M Koo. *Physica B: Condensed Matter*, 322(34):236 – 247, 2002. doi: http://dx.doi.org/10.1016/S0921-4526(02)01188-2. URL http://www.sciencedirect.com/science/article/pii/S0921452602011882.

[66] C.G. Schull and M.K. Wilkinson. *Phys. Rev.*, 97:305, 1955.

[67] Shun-Li Shang, Yi Wang, Yong Du, and Zi-Kui Liu. *Intermetallics*, 18(5):961 – 964, 2010. ISSN 0966-9795. doi: http://dx.doi.org/10.1016/j.intermet.2010.01.011. URL http://www.sciencedirect.com/science/article/pii/S0966979510000221.

[68] R. E. Parra and J. W. Cable. *Phys. Rev. B*, 21:5494–5504, Jun 1980. doi: 10.1103/PhysRevB.21.5494. URL http://link.aps.org/doi/10.1103/PhysRevB.21.5494.

[69] A. Aguayo, I. I. Mazin, and D. J. Singh. *Phys. Rev. Lett.*, 92:147201, Apr 2004. doi: 10.1103/PhysRevLett.92.147201. URL http://link.aps.org/doi/10.1103/PhysRevLett.92.147201.

[70] F. R. de Boer, C. J. Schinkel, J. Biesterbos, and S. Proost. *Journal of Applied Physics*, 40(3):1049–1055, 1969. doi: http://dx.doi.org/10.1063/1.1657528. URL http://scitation.aip.org/content/aip/journal/jap/40/3/10.1063/1.1657528.

[71] A. J. Cox, , J. G. Louderback, and L. A. Bloomfield. *Phys. Rev. Lett.*, 71:923–926, Aug 1993. doi: 10.1103/PhysRevLett.71.923. URL http://link.aps.org/doi/10.1103/PhysRevLett.71.923.

[72] H. Chen, N. E. Brener, and J. Callaway. *Phys. Rev. B*, 40:1443–1449, Jul 1989. doi: 10.1103/PhysRevB.40.1443. URL http://link.aps.org/doi/10.1103/PhysRevB.40.1443.

[73] L. Ortenzi, I. I. Mazin, P. Blaha, and L. Boeri. *Phys. Rev. B*, 86:064437, Aug 2012. doi: 10.1103/PhysRevB.86.064437. URL http://link.aps.org/doi/10.1103/PhysRevB.86.064437.

[74] J. Koßmann, T. Hammerschmidt, S. Maisel, S. Müller, and R. Drautz. *Intermetallics*, 64:44–50, 2015. doi: 10.1016/j.intermet.2015.04.009.

[75] M. Balarin and K. Bartsch. *Zeitschrift fr anorganische und allgemeine Chemie*, 622 (5):919–921, 1996. doi: 10.1002/zaac.19966220529. URL http://dx.doi.org/10.1002/zaac.19966220529.

[76] Y. Mishin, M.J. Mehl, and D.A. Papaconstantopoulos. *Acta Materialia*, 53 (15):4029 – 4041, 2005. doi: http://dx.doi.org/10.1016/j.actamat.2005.05.001. URL http://www.sciencedirect.com/science/article/pii/S1359645405002843.

[77] A. Stephen, F. Rossi, L. Nasi, C. Ferrari, N. Ponpandian, M. Ananth V., and V. Ravichandran. *Journal of Applied Physics*, 103(5):053511, 2008. doi: http://dx.doi.org/10.1063/1.2844211. URL http://scitation.aip.org/content/aip/journal/jap/103/5/10.1063/1.2844211.

[78] M. Sanati, L. G. Wang, and A. Zunger. *Phys. Rev. Lett.*, 90:045502, Jan 2003. doi: 10.1103/PhysRevLett.90.045502. URL http://link.aps.org/doi/10.1103/PhysRevLett.90.045502.

[79] Y. Wang, Z.-K. Liu, and L.-Q. Chen. *Acta Materialia*, 52(9):2665 – 2671, 2004. doi: http://dx.doi.org/10.1016/j.actamat.2004.02.014. URL http://www.sciencedirect.com/science/article/pii/S1359645404000965.

[80] Xiang He, Wen-Chao Wang, and Bai-Xin Liu. *Phys. Rev. B*, 77:012401, Jan 2008. doi: 10.1103/PhysRevB.77.012401. URL http://link.aps.org/doi/10.1103/PhysRevB.77.012401.

[81] E.T. Peters and L.E. Tanner. *Trans. Met. Soc. AIME*, 233:2126–2128, 1965.

[82] Y. Aoki, K. Asami, and M. Yamamoto. *physica status solidi (a)*, 23(2):K167–K169, 1974. ISSN 1521-396X. doi: 10.1002/pssa.2210230260. URL http://dx.doi.org/10.1002/pssa.2210230260.

[83] Y. Aoki and J. Echigoya. *Scripta Metallurgica*, 19(5):639 – 642, 1985. ISSN 0036-9748. doi: http://dx.doi.org/10.1016/0036-9748(85)90352-7. URL http://www.sciencedirect.com/science/article/pii/0036974885903527.

[84] L. J. Nagel, B. Fultz, and J. L. Robertson. *Journal of Phase Equilibria*, 18:21, 1997. doi: 10.1007/BF02646756. URL http://dx.doi.org/10.1007/BF02646756.

[85] Sri Raghunath Joshi, K.V. Vamsi, and S. Karthikeyan. *MATEC Web of Conferences*, 14:18001, 2014. doi: 10.1051/matecconf/20141418001. URL http://dx.doi.org/10.1051/matecconf/20141418001.

[86] James E. Saal and C. Wolverton. *Acta Materialia*, 61(7):2330 – 2338, 2013. ISSN 1359-6454. doi: http://dx.doi.org/10.1016/j.actamat.2013.01.004. URL http://www.sciencedirect.com/science/article/pii/S135964541300013X.

[87] Robert K. Rhein, Philip C. Dodge, Min-Hua Chen, Michael S. Titus, Tresa M. Pollock, and Anton Van der Ven. *Phys. Rev. B*, 92:174117, Nov 2015. doi: 10.1103/PhysRevB.92.174117. URL http://link.aps.org/doi/10.1103/PhysRevB.92.174117.

[88] Satoru Kobayashi, Yuki Tsukamoto, and Takayuki Takasugi. *Intermetallics*, 31:94 – 98, 2012. ISSN 0966-9795. doi: http://dx.doi.org/10.1016/j.intermet.2012.06.006. URL http://www.sciencedirect.com/science/article/pii/S0966979512002208.

[89] George Vassilev Penev, Tomas Gomez-Acebo, and Jean-Claude Tedenac. *Journal of Phase Equilibria*, 21(3):287–301, 2000. ISSN 1054-9714. doi: 10.1361/105497100770340075. URL http://dx.doi.org/10.1361/105497100770340075.

[90] J. M. Cowley. *Journal of Applied Physics*, 21:24–30, 1950. doi: http://dx.doi.org/10.1063/1.1699415. URL http://scitation.aip.org/content/aip/journal/jap/21/1/10.1063/1.1699415.

[91] B.E. Warren. *X-ray diffraction*. New York, Dover, United States, 1990.

[92] N. M. Rosengaard and H. L. Skriver. *Phys. Rev. B*, 50:4848–4858, 1994. doi: 10.1103/PhysRevB.50.4848. URL http://link.aps.org/doi/10.1103/PhysRevB.50.4848.

[93] J. B. Liu and D. D. Johnson. *Materials Research Innovations*, 18:S4–1021–S4–1025, 2014. doi: 10.1179/1432891714Z.000000000872. URL http://dx.doi.org/10.

1179/1432891714Z.000000000872.

[94] P. Veyssiére, J. Douin, and P. Beauchamp. *Philosophical Magazine A*, 51(3):469–483, 1985. doi: 10.1080/01418618508237567. URL http://dx.doi.org/10.1080/01418618508237567.

[95] I. Baker, R. Darolia, and J. D. Whittenberger, editors. Materials Research Society Symposium Proceedings No. 288, Boston, Massachusetts, USA, 1993. Materials Research Society.

[96] A. T. Paxton. Point, line and planar defects. In D. G. Pettifor and A. H. Cottrell, editors, *Electron Theory in Alloy Design*, page 158. The Institute of Materials, London, 1992.

[97] G. M. Stocks, D. P. Pope, and A. F. Giamei, editors. Materials Research Society Symposium Proceedings No. 186, Pittsburgh, USA, 1991. Materials Research Society.

[98] O.N. Mryasov, Yu.N. Gornostyrev, M. van Schilfgaarde, and A.J. Freeman. *Acta Materialia*, 50(18):4545 – 4554, 2002. ISSN 1359-6454. doi: http://dx.doi.org/10.1016/S1359-6454(02)00282-3. URL http://www.sciencedirect.com/science/article/pii/S1359645402002823.

[99] Yu feng Wen, Jian Sun, and Jian Huang. *Transactions of Nonferrous Metals Society of China*, 22(3):661 – 664, 2012. doi: http://dx.doi.org/10.1016/S1003-6326(11)61229-6. URL http://www.sciencedirect.com/science/article/pii/S1003632611612296.

[100] V. Paidar, D.P. Pope, and M. Yamaguchi. *Scripta Metallurgica*, 15(9):1029 – 1031, 1981. doi: http://dx.doi.org/10.1016/0036-9748(81)90248-9. URL http://www.sciencedirect.com/science/article/pii/0036974881902489.

[101] J.B. Liu, D.D. Johnson, and A.V. Smirnov. *Acta Materialia*, 53(13):3601 – 3612, 2005. doi: http://dx.doi.org/10.1016/j.actamat.2005.04.011. URL http://www.sciencedirect.com/science/article/pii/S1359645405002260.

[102] T. Takasugi, S. Hirakawa, O. Izumi, S. Ono, and S. Watanabe. *Acta Metallurgica*, 35(8):2015 – 2026, 1987. doi: http://dx.doi.org/10.1016/0001-6160(87)90030-7. URL http://www.sciencedirect.com/science/article/pii/0001616087900307.

[103] G. Vanderschaeve. *Philosophical Magazine A*, 56(6):689–701, 1987. doi: 10.1080/01418618708204482. URL http://dx.doi.org/10.1080/01418618708204482.

[104] P. Veyssière. Properties of surface defects in intermetallics. In C. T. Liu, R. W. Cahn, and G. Sauthoff, editors, *Ordered Intermetallics — Physical Metallurgy and Mechanical Behaviour*, pages 165–175. Springer Netherlands, Dordrecht, 1992. ISBN 978-94-011-2534-5. doi: 10.1007/978-94-011-2534-5_13. URL http://dx.doi.org/10.1007/978-94-011-2534-5_13.

[105] Yi Liu, Takayuki Takasugi, Osamu Izumi, and Takeshi Takahashi. *Philosophical Magazine A*, 59:423–436, 1989. doi: 10.1080/01418618908205067. URL http://www.tandfonline.com/doi/abs/10.1080/01418618908205067.

[106] D.M. Wee, D.P. Pope, and V. Vitek. *Acta Metallurgica*, 32:829 – 836, 1984. ISSN 0001-6160. doi: http://dx.doi.org/10.1016/0001-6160(84)90019-1. URL http://www.sciencedirect.com/science/article/pii/0001616084900191.

[107] Y Wang, J J Wang, H Zhang, V R Manga, S L Shang, L-Q Chen, and Z-K Liu. *Journal of Physics: Condensed Matter*, 22(22):225404, 2010. URL http://stacks.iop.org/0953-8984/22/i=22/a=225404.

[108] Shun-Li Shang, Hui Zhang, Yi Wang, and Zi-Kui Liu. *Journal of Physics: Condensed Matter*, 22(37):375403, 2010. URL http://stacks.iop.org/0953-8984/22/i=37/a=375403.

[109] C.A. Swenson. *Journal of Physics and Chemistry of Solids*, 29(8):1337 – 1348, 1968. ISSN 0022-3697. doi: http://dx.doi.org/10.1016/0022-3697(68)90185-6. URL http://www.sciencedirect.com/science/article/pii/0022369768901856.

[110] E.F. Wasserman. Chapter 3 invar: Moment-volume instabilities in transition metals and alloys. In *Handbook of Ferromagnetic Materials*, volume 5 of *Handbook of Ferromagnetic Materials*, pages 237 – 322. Elsevier, 1990. doi: http://dx.doi.org/10.1016/S1574-9304(05)80063-X. URL http://www.sciencedirect.com/science/article/pii/S157493040580063X.

[111] Orson L. Anderson and Donald G. Isaak. *Elastic Constants of Mantle Minerals at High Temperature*, pages 64–97. American Geophysical Union, 2013. ISBN 9781118668191. doi: 10.1029/RF002p0064. URL http://dx.doi.org/10.1029/RF002p0064.

[112] I. Bleskov, T. Hickel, J. Neugebauer, and A. Ruban. *Phys. Rev. B*, 93:214115, Jun 2016. doi: 10.1103/PhysRevB.93.214115. URL http://link.aps.org/doi/10.1103/PhysRevB.93.214115.

[113] Vsevolod I. Razumovskiy, Andrei Reyes-Huamantinco, Peter Puschnig, and A. V. Ruban. *Phys. Rev. B*, 93:054111, Feb 2016. doi: 10.1103/PhysRevB.93.054111. URL `http://link.aps.org/doi/10.1103/PhysRevB.93.054111`.